Elsevier Editorial System(tm) for The International Journal of Biochemistry & Cell Biology

Manuscript Draft

Manuscript Number: BC-D-14-00215R1

Title: Homeobox b5 (Hoxb5) regulates the expression of Forkhead box D3 gene (Foxd3) in neural crest

Article Type: Regular Research Article

Keywords: Hoxb5; Foxd3; neural crest; transcription; survival

Corresponding Author: Dr. Vincent Chi Hang Lui, Ph.D.

Corresponding Author's Institution: The University of Hong Kong

First Author: Mandy K Kam, Ph.D.

Order of Authors: Mandy K Kam, Ph.D.; Martin Cheung, Ph.D.; Joe J Zhu, Ph.D.; William W Cheng, Ph.D.; Eric W Sar; Paul K Tam, M.D.; Vincent Chi Hang Lui, Ph.D.

Manuscript Region of Origin: HONG KONG

**Homeobox b5 (Hoxb5) regulates the expression of Forkhead box D3 gene (*Foxd3*) in neural crest**

Mandy Ka Man Kam,[1] Martin Cheung,[2,3] Joe Jiang Zhu,[1,4] William Wai Chun Cheng,[1] Eric Wai Yin Sat,[1] Paul Kwong Hang Tam[1,3] and Vincent Chi Hang Lui[1,3]

[1]Department of Surgery, [2]Department of Anatomy, [3]Centre for Reproduction, Development & Growth, Li Ka Shing Faculty of Medicine, The University of Hong Kong, 21 Sassoon Road, Pokfulam, Hong Kong, China. [4]Faculty of Medicine, Shenzhen University, Shenzhen, Guangdong Province, China.

Address correspondence to:

Vincent Chi Hang Lui, Department of Surgery, Li Ka Shing Faculty of Medicine, The University of Hong Kong, 21 Sassoon Road, Pokfulam, Hong Kong, China.

Phone: (852)28199607

Fax: (852)28199621

Email: vchlui@hku.hk

Running title: Hoxb5 regulates *Foxd3* expression

Keywords: *Hoxb5*; *Foxd3*; neural crest; transcription; survival

Conflict of interest: The authors declare that there are no conflicts of interest with respect to authorship and/or publication of this article.

**Abstract**

Patterning of neural crest (NC) for the formation of specific structures along the anterio-posterior (A-P) body axis is governed by a combinatorial action of *Hox* genes, which are expressed in the neuroepithelium at the time of NC induction. *Hoxb5* was expressed in NC at both induction and migratory stages, and our previous data suggested that *Hoxb5* played a role in the NC development. However, the underlying mechanisms by which Hoxb5 regulates the early NC development are largely unknown. Current study showed that both the human and mouse *Foxd3* promoters were bound and trans-activated by Hoxb5 in NC-derived neuroblastoma cells. The binding of Hoxb5 to *Foxd3* promoter *in vivo* was further confirmed in the brain and neural tube of mouse embryos. Moreover, *Wnt1-Cre* mediated perturbation of Hoxb5 signaling at the dorsal neural tube in mouse embryos resulted in *Foxd3* down-regulation. *In ovo*, Foxd3 alleviated the apoptosis of neural cells induced by perturbed Hoxb5 signaling, and Hoxb5 induced ectopic *Foxd3* expression in the chick neural tube. This study demonstrated that *Hoxb5* (an A-P patterning gene) regulated the NC development by directly inducing *Foxd3* (a NC specifier and survival gene).

## 1. Introduction

The neural crest (NC) belongs to a transient, multipotent stem-cell population arising from the interface between the neural plate and the non-neural ectoderm upon the induction by extrinsic factors including the bone morphogenetic proteins, fibroblast growth factors, Wnt and retinoic acid emanating from the non-neural ectoderm or the non-axial mesoderm (Stuhlmiller and Garcia-Castro 2012). In response to these molecules, dorsal neural fold acquires competence by expressing a number of neural plate border genes which in turn induce a set of NC specifiers such as *Snail2*, *Foxd3* and *Sox9* to establish the NC identity (Knecht and Bronner-Fraser 2002; Meulemans and Bronner-Fraser 2004). The molecular cascades of signaling inputs, neural plate border genes and NC specifiers form a complex gene regulatory network (GRN) that orchestrates the NC ontogeny.

Homeobox (*Hox*) genes play an essential role in the NC patterning along the anterio-posterior (A-P) axis, however, little is known about the direct interaction between the *Hox* genes and the GRN. Loss- and gain-of-function experiments in mice revealed that *Hox* genes executed their regulatory functions by specifying the NC-derived structures corresponding to their expressions at a given A-P level (Mallo et al. 2010). For example, the deletion of *Hox* genes (*Hox1* to *Hox4*) with anterior expression boundaries resulted in NC developmental defects in the regions, indicating that these *Hox* genes regulated the differentiation of cranial NC (Gendron-Maguire et

al. 1993; Kessel 1993; Rijli et al. 1993; Gavalas et al. 1998; Studer et al. 1998). *Foxd3* was identified to be a downstream target of *Hoxa1* in the cardiac NC development, suggesting that anterior *Hox* gene could interact with the GRN in the cardiac NC which emigrated from the anterior axis of the neural tube (Makki and Capecchi 2011). Because of the overlapping expression domains at the progressively posterior axis of the neural tube and the extensive functional redundancy among the *Hox* members, single or multiple knockout of the posterior *Hox* genes failed to reveal any NC developmental defects. Recent studies in chick showed that electroporation of *Hoxb1* into the posterior neural tube of chick embryo resulted in ectopic expression of *Snail2* and *Msx1*/*2*, and an induction of neural progenitors to NC fate accompanied by an epithelial mesenchymal transition (EMT) (Gouti et al. 2011). However, single or combined electroporation of *Snail2* and *Msx1*/*2* were all insufficient to induce an EMT in the trunk NC (del Barrio and Nieto 2002; Nieto 2002). In addition, Bmp and Notch signaling were required for the NC induction by *Hoxb1* (Gouti et al. 2011). These findings suggested that *Hoxb1*, an anterior patterning gene, interacted with the GRN modules and the signaling pathways to induce NC formation. Whether the posterior *Hox* genes also interact with the components of the GRN is not clear.

One of the posterior *Hox* genes, *Hoxb5*, was expressed in the neuroepithelium from the myelencephalon to the posterior end of the neural tube, with the highest

expression domain spanning from the myelencephalon to the vagal level of the neural tube (Krumlauf et al. 1987; Hogan et al. 1988; Holland and Hogan 1988; Kuratani and Wall 1992; Wall et al. 1992). *Hoxb5* was expressed in human, mouse and chick dorsal neural tube at the time of NC induction (Knecht and Bronner-Fraser 2002; Cheung et al. 2005), and later in the migratory NC (Holland and Hogan 1988; Kuratani and Wall 1992; Wall et al. 1992; Fu et al. 2003). Deletion of *Hoxb5* resulted in an A-P patterning defect of the shoulder girdle in mice without affecting NC-derived tissues (Rancourt et al. 1995). The lack of defects in NC and their derived tissues in *Hoxb5*$^{-/-}$ mice could be due to the functional redundancy among paralogous *Hox* members. For instance, *Hoxa5*, *Hoxb5* and *Hoxc5* were shown to function in a redundant manner in the developing murine forelimb (Xu et al. 2013) and lung (Boucherat et al. 2013). To circumvent the functional redundancy problem and investigate the function of *Hoxb5* in the NC development, we generated mice (*enb5*;*Wnt1-Cre*) that expressed a dominant negative chimeric protein, engrailed-Hoxb5 (enb5), upon Cre-induction. This enb5 repressor competed with Hoxb5 for the binding to target genes, thereby disrupting its developmental pathways. Using *enb5*;*Wnt1-Cre* mice, we previously showed that Hoxb5 bound to the promoter of *Sox9* and regulated its expression in the trunk NC, and perturbation of Hoxb5 function by enb5 caused down-regulation of *Sox9* and apoptosis of the pre-migratory and migratory NC (Kam et al. 2014).

*Foxd3* encodes a transcriptional factor of the winged helix or Forkhead family proteins (Sutton et al. 1996; Labosky and Kaestner 1998). *Foxd3* was strongly expressed in the pre-migratory NC at the head fold of embryonic mouse at E8.0, its expression extended to the migratory vagal NC from E9.0 onwards (Mundell and Labosky 2011). *Foxd3* positive cells were later found in multiple developing NC derivatives in the E11.5 mouse embryos (Mundell and Labosky 2011). Deletion of *Foxd3* in *Foxd3*$^{flox/-}$;*Wnt1-Cre* mice led to the apoptosis of NC and developmental defects of multiple NC-derived structures including the palate, the peripheral nervous system (PNS) and the enteric nervous system (ENS) (Teng et al. 2008). NC apoptosis, developmental defects of the PNS and ENS were also reported in the *enb5;Wnt1-Cre* mice (Kam et al. 2014), which prompted us to interrogate if (a) Hoxb5 regulated *Foxd3* expression in the NC, and (b) the developmental defects in *enb5;Wnt1-Cre* mice were attributed to a reduction of *Foxd3* expression in the NC.

In this study, *in silico* analysis revealed putative Hoxb5 binding sites in the promoters of the human and mouse *Foxd3* gene; subsequent assays confirmed that the *Foxd3* promoter was bound and trans-activated by Hoxb5. The *Foxd3* expression of mouse neural tube was reduced when Hoxb5 function was perturbed in the *enb5;Wnt1-Cre* mice. In chick neural tube, the apoptosis caused by *enb5* was alleviated by *Foxd3*, and *Hoxb5* induced ectopic *Foxd3* expression. In conclusion, our

findings demonstrated that *Hoxb5*, a member of A-P patterning gene family, directly induced the expression of *Foxd3* and regulated the survival of NC at the early NC development.

## 2. Materials and Methods

### *2.1. Mouse lines*

The *enb5* (Lui et al. 2008) and *Wnt1-Cre* (kindly provided by Prof. Andrew P McMahon, Harvard University, USA) mice were respectively maintained in the (*BLK6/CBA*) F1 Hybrid and *ICR* genetic backgrounds. The *Wnt1-Cre* and *enb5* genotyping by PCR was performed as previously described (Lui et al. 2008; Kam et al. 2014). Embryo was designated as embryonic day (E) 0.5 by the detection of the vaginal plug. All the experimental procedures were approved by the Committee on the Use of Live Animals at the University of Hong Kong (CULATR 2038-009).

### *2.2. Reagents*

Antibodies were obtained from the following sources: FLAG (Sigma, St. Louis, MO USA; catalogue no. F3165), Foxd3 (gift from Prof. Patricia A Labosky, Vanderbilt University Medical Center; 1:1000); GFP (AbDirect, Oxford, UK; catalogue no. 4745-1051, 1:1000); Hoxb5 (Santa Cruz Biotechnology Inc., Dallas, Texas USA; catalogue no. sc-82895 or sc-81099). The plasmids for riboprobe synthesis were obtained from the following sources: mouse *Foxd3* from Dr. Ruth Arkell (Laboratory of Early Development, Mammalian Genetics Unit, MRC, Harwell, UK) and chick *Foxd3* from BBSRC Chick EST bank *Foxd3* (I.M.A.G.E. ID 418507); the plasmids for chick *in ovo* electroporation: full length cDNA of chick *Hoxb5* and *enb5* were

cloned into the *pCIG* expression vector (Niwa et al. 1991).

### *2.3. TUNEL assay and immuno-fluorescence staining*

TUNEL assay and immunofluorescence staining for GFP were performed as described previously (Kam et al. 2014). Images were taken with Nikon Eclipse 80i microscope (Melville, NY, USA) mounted with SPOT RT3 microscope digital camera (DIAGNOSTIC instruments, Inc. Sterling Heights, USA). Photos were compiled using Adobe Photoshop 7. To quantitate the number of transfected cells that underwent apoptosis within the chick neural tube, the apoptotic (TUNEL+ve and GFP+ve cells) and non-apoptotic (TUNEL–ve and GFP+ve) transfected neural cells on sections were counted. Five neural tubes respectively electroporated with *enb5* or *enb5+Foxd3*; and at least three sections of each neural tube were counted. The average percentage of apoptotic cells among transfected neural cells in each group (EP: *enb5* and *enb5+Foxd3*) was calculated and shown as mean±SEM.

### *2.4. Immuno-fluorescence staining on paraffin sections*

Embryos were fixed in 4% paraformaldehyde (w/v) in PBS (PFA/PBS) for overnight at 4°C, dehydrated and embedded in paraffin wax. Paraffin sections of 8 μm were prepared and mounted onto TESPA-coated glass slides. Antigen retrieval was performed by incubating in sodium citrate buffer (10mM; pH6.0) at 95°C for 45 minutes. The sections were then blocked in 0.5% Blocking reagent (Roche Applied

Science, Indianapolis, IN, USA), 3% Normal goat serum (Invitrogen), 3% Normal sheep serum (Invitrogen), 3% Fetal bovine serum (HyClone) in PBS, 0.1% Triton for 2 hours before being incubated overnight at 4°C with antibody for Foxd3. After washing in PBS, the sections were incubated with anti-rabbit AlexaFlour® 488-conjugated secondary antibodies (Invitrogen; A-11008; 1:200) at room temperature for 2 hours. After washing with PBS (0.1% Triton) and dehydration in alcohol, the sections were mounted in DAPI containing anti-fade solution (Vector Laboratories., Inc.). Images were taken with Nikon Eclipse 80i microscope (Melville, NY, USA) mounted with SPOT RT3 microscope digital camera (DIAGNOSTIC instruments, Inc. Sterling Heights, USA). Photos were compiled using Adobe Photoshop 7. The migratory Foxd3 immuno-positive NC in the trunk regions of the *enb5*;*Wnt1-Cre* mutant and *enb5* wild-type control mice were quantitated by counting the Foxd3+ve cells on the respective transverse sections. Eight embryos of each group were examined and at least three serial sections of each embryo were counted. The number of migratory Foxd3+ve cells on the sections of *enb5*;*Wnt1-Cre* and *enb5* mice was calculated and shown as mean±SD.

### *2.5. In situ hybridization*

DIG-labeled riboprobes were synthesized according to the manufacturer's protocol (Roche Applied Science, Indianapolis, IN, USA). *In situ* hybridization was performed

on mouse embryos and frozen sections of chick embryos to detect the expression of *Foxd3* as previously described (Kam et al. 2014). Photographs of embryos were taken on an Olympus SZX7 microscope fitted with an Olympus digital camera DP7 under bright-field illumination.

### *2.6. Chromatin immuno-precipitation assay (ChIP) and quantitative PCR assay*

ChIP was performed using Pierce Agarose ChIP Kit (Thermo Fisher Scientific, Rockland, USA) according to the manufacturer's instructions. ChIP assay on (a) the human neuroblastoma cell line SK-N-SH (#HTB-11) (ATCC, Manassas, USA) transfected with *HOXB5* or *Flag-enb5* (Zhu et al. 2011), and (b) the mouse developing central nervous system were performed as previously described (Kam et al. 2014). The binding of *FOXD3* promoter sequences to HOXB5 and Flag-enb5 was quantified by quantitative PCR analysis. The primers for human and mouse *FOXD3* promoter sequences: *ChIP_FOXD3F1* (5'-CTG ACG TCA CGC ACG GTC ACG-3') and *ChIP_FOXD3R3* (5'-CCC GGT AGT CGA AAG TCC CGT TT-3'). Quantitative PCR was performed on 7900HT Fast Real-Time PCR System using Fast SYBR Green Master Mix (Applied Biosystems, Foster City, USA).

### *2.7. Quantitative RT-PCR*

Ten neural tubes of the E9.5 *enb5*;*Wnt1-Cre* and *enb5* mice were dissected, and pooled for RNA extractions with Trizol (Life Technologies, CA, US) following the

manufacturer's instruction. First strand cDNA was synthesized by using Reverse Transcription System (Promega). Quantitative PCR was performed on 7900HT Fast Real-Time PCR System using Fast SYBR Green Master Mix (Applied Biosystems, Foster City, USA), and were performed in triplicate. The primers for *Foxd3*: Forward: (5'-CCA GGC GGT ACG CCC TCT CT-3'); Reverse: (5'-GGG GAT GGA GGC CGC TGT TG-3'); the primers for *18S*: Forward; (5"-CGG CTA CCA CAT TCC AAG GA-3'); Reverse: (5'-GCT GGA ATT ACC GCG GCT-3'). The quantitative RT-PCR analysis was repeated on the RNAs isolated from a second batch of mutant and control embryos as biological replicates. Therefore, a total of 20 neural tubes of the E9.5 *enb5*;*Wnt1-Cre* and *enb5* mice were included for the quantitative PCR analysis. The relative expression levels of *Foxd3* to *18S* (internal control) were calculated by using ΔCT method. The relative expression of *Foxd3* in both groups was shown as mean±SEM; with that of enb5 wild-type control group was taken arbitrarily as one.

### *2.8. Electro-mobility shift assay (EMSA)*

PCR products spanning the putative HOX binding sites of the human *FOXD3* promoter were labeled with Biotin-11-UTP (Pierce, Thermo Fisher Scientific, Rockland, USA). The incubation of biotin-labeled DNA fragment with GST-HOXB5 protein (Abnova, Taipei, H-00003215-Q01) with or without the addition of unlabeled

fragment as a specific competitor, electrophoresis and visualization of retarded probes by chemiluminescence were performed as previously described (Zhu et al. 2011).

### *2.9. Transient transfection and dual-luciferase reporter assay*

The 666 bp (-927 to -261) human *FOXD3*-lucifrease reporting vector [*FOXD3* (*wt*)-*Luc*] was kindly provided by Prof. Richard A. Spritz (University of Colorado Denver, Aurora, USA) (Alkhateeb et al. 2005). Mutated form of the human *FOXD3* promoter with the deletion of the predicted HOX binding site (-511 to -495), *FOXD3* (*del*)-*Luc* was generated using QuikChange® Site-Directed Mutagenesis Kit according to the manufacturer's protocol (Stratagene, Santa Clara, CA, USA). The dual-luciferase reporter assay was performed as previously described (Zhu et al. 2011) with the use of *HOXB5*, *enb5* and *FLAG-enb5* expression vectors in different combinations (50ng each; appropriate amount of *pRC*/*CMV* empty vector was added to the transfection mixture to keep the total amount of the expression vectors at 150ng) together with the reporter construct (250ng) and pRL internal control (2ng). At least two independent triplicate or quintuplicate experiments were performed, and the luciferase activity was presented as relative luciferase unit (RLU) normalized with the Renilla luciferase internal control.

### *2.10. Chick in ovo electroporation*

Fertilized chick eggs were obtained from SIPAFASI (Jinan, China), the staging of

embryos and the electroporation of chick neural tube were performed as previously described (Kam et al. 2014).

### *2.11. Statistical analyses*

ANOVA was performed for all experiments to calculate the differences between groups, and $p$ value $<0.05$ was regarded as statistically significant.

## 3. Results

### *3.1. HOXB5 bound and trans-activated FOXD3 promoter*

*In silico* analysis predicted a putative HOX binding site (AGTAATCTATCAGGCC) spanning from -531 to -546 at the 5' upstream of the transcription start site of the human *FOXD3* promoter (Figure 1A). To further evaluate if HOXB5 bound to the putative binding site of the human *FOXD3* gene, electro-mobility shift assay (EMSA) and chromatin immuno-precipitation (ChIP) assay were performed. As revealed by EMSA, a retarded band was observed only in the lane containing the GST-HOXB5 and the biotin-labeled oligonucleotide probe (spanning from -521 to -575; Figure 1A) that encompassed the putative HOX binding sequence. The intensity of the retarded band was markedly reduced if excess unlabeled oligonucleotide (Cold probe) was included in the reaction mixtures. No retarded band was observed if the GST-HOXB5 was replaced with the GST protein. More importantly, deletion of the core binding sequence (-531 to -546) from the probe (*FOXD3 (del)*) abolished the specific binding between the GST-HOXB5 and the probe. Next, we extended this analysis by looking at the binding of HOXB5 to the *FOXD3* promoter in a human neuroblastoma cell line (SK-N-SH) transfected with *HOXB5*, using ChIP followed by quantitative PCR. Binding of HOXB5 to the *FOXD3* promoter was significantly enriched by 2.65±0.13 (mean±SEM) folds as compared to the non-specific IgG control (Figure 1C).

To test if HOXB5 protein trans-activated the *FOXD3* promoter, we transfected a luciferase reporter construct (*FOXD3 (wt)-Luc*) consisting of 666 bp (-927 to -261) of the human *FOXD3* gene 5' of the luciferase gene into SK-N-SH cells. Co-transfection of *HOXB5* enhanced the transcription by 10.35±0.25 (mean±SD) folds compared to the *pRC/CMV* control (Figure 1D). Deletion of the HOXB5 core binding sequence (-536 to -542) from the *FOXD3* promoter (*FOXD3 (del)-Luc*) reduced the induction to 2.81±0.03 (mean±SD) folds. Our data revealed that the binding of HOXB5 to the *FOXD3* promoter increased the transcription from the *FOXD3* promoter.

Sequence comparison revealed a marked similarity between the human and the mouse *FOXD3* promoters and a putative HOX binding sequence was also located in the mouse promoter (Figure 2A). ChIP assay on the chromatin prepared from the E9.5 mouse brain and neural tube showed a 3.06±0.16 (mean±SEM) folds of enrichment, confirming the *in vivo* binding of Hoxb5 to *Foxd3* promoter (Figure 2B).

### *3.2. HOXB5 induction of FOXD3 was reduced by the dominant negative chimeric protein, engrailed-Hoxb5 (enb5)*

The chimeric protein namely enb5 which contained the *Drosophila* engrailed repressor domain and the DNA binding domain of the mouse Hoxb5, competed with Hoxb5 for binding to target genes and interfered with the normal Hoxb5 function (Lui et al. 2008; Kam et al. 2014). Transfection of this dominant-negative form of Hoxb5,

markedly suppressed the trans-activation of *FOXD3* by HOXB5 in SK-N-SH cells (Figure 3A). Due to the unavailability of anti-enb5 protein for ChIP assay, a vector expressing a Flag-tagged enb5 (Flag-enb5) with the FLAG epitope (N'-DYKDDDDK-C') at the N-terminus was generated to test the mechanism of the suppression. Flag-enb5 suppressed the HOXB5-transactivated *FOXD3* promoter activity by 55±6% (mean±SD) in SK-N-SH cells (Figure 3B). ChIP and quantitative PCR analysis revealed a 5.51±0.18 (mean±SEM) folds of enrichment as compared to the non-specific IgG control, suggesting that Flag-enb5 (and therefore enb5) bound to the same regions of the *FOXD3* promoter as HOXB5 (Figure 3C). Taken together, our *in vitro* data indicated that HOXB5 bound to the *FOXD3* promoter and its dominant-negative chimera, enb5, suppressed the HOXB5 induction.

### *3.3. Perturbation of Hoxb5 function caused down-regulation of Foxd3 in mice*

The expression of enb5, the dominant negative chimeric protein of Hoxb5, in NC by *Wnt1-Cre* resulted in apoptotic depletion of pre-migratory and early migratory NC in mice (Kam et al. 2014). These *enb5*;*Wnt1-Cre* mice displayed developmental defects of trunk NC-derived tissues including hypoplasia of DRG and absence of enteric neuroblasts in the gut (Kam et al. 2014), which were also observed in the *Foxd3*$^{flox/-}$;*Wnt1-Cre* mice (Teng et al. 2008).

To test if the perturbation of Hoxb5 function reduced the *Foxd3* expression in the

*enb5*;*Wnt1-Cre* mice, we performed whole-mount *in situ* hybridization for *Foxd3* in the *enb5*;*Wnt1-Cre* and the *enb5* embryos. In the E9.5 *enb5* embryos, *Foxd3* transcripts were detected in the hindbrain and in the dorsal neural tube (Figure 4A). By E10.5, *Foxd3* expression was extended to the midbrain and in the forelimb bud (Figure 4C). Transcripts of *Foxd3* were detected in the similar regions in the *enb5*;*Wnt1-Cre* embryos; however, the intensity of the staining was generally weaker (Figure 4A, C). Expression of *Foxd3* in the neural tube of the E9.5 *enb5*;*Wnt1-Cre* embryos was significantly reduced by 0.50±0.05 (mean±SEM) fold as compared to that in the neural tube of the *enb5* embryos (Figure 4B). In the E9.5 *enb5* embryos, Foxd3-expressing NC were localized at the dorsal neural tube, along the dorsal-lateral migration pathway under the surface ectoderm and ventral-medial migration pathway to the cardinal vein (Figure 4D). Although Foxd3 immuno-positive NC were similarly located along the NC migration pathway, number of Foxd3-expressing NC was much fewer in the *enb5*;*Wnt1-Cre* mice (Figure 4D). The number of migratory NC in the trunk region of the E9.5 neural tube was statistically lower in the *enb5*;*Wnt1-Cre* embryos (24±2 (mean±SD) (n=8)) than that in the *enb5* embryos (54.7±7 (mean±SD) (n=8)) (Figure 4E).

### *3.4. Foxd3 alleviated enb5-induced cell death and Hoxb5 induced Foxd3 expression in ovo*

The electroporation of HH10-11 chick neural tube with *enb5* induced massive cell death in the transfected region but only a few apoptotic cells were detected in the contralateral non-electroporated side (Figure 5A). Co-electroporation of *Foxd3* notably reduced the enb5-induced cell death (Figure 5A). Percentage of the transfected neural tube cells (GFP+ve) undergoing apoptosis (TUNEL+ve) in the chick neural tubes electroporated with *enb5* alone (49.4±7.5% (mean±SEM); n=5) was statistical significantly higher than those co-electroporated with *Foxd3* (15.6±4.3 (mean±SEM); n=5) (Figure 4B). When the chick neural tubes were electroporated with the chick *Hoxb5* expressing vector, ectopic expression of *Foxd3* was observed in the dorsal part of the neural tube of the electroporated side 12 hours after transfection (Figure 5C).

## 4. Discussion

Neural crest (NC) ontogeny is orchestrated by the interplay between signaling molecules, neural plate border genes and NC specifiers that form a complex gene regulatory network (GRN). The establishment of A-P position identity to imbue the ability of NC to differentiate into specific structures is controlled by a combinatorial action of *Hox* genes. However, little is known about how *Hox* genes genetically interact with the GRN to regulate the early NC development. In the current study, we report that *Hoxb5*, in addition to its A-P patterning role, also plays critical roles in regulating the NC development by directly trans-activating the expression of a NC specifier and survival gene, *Foxd3*.

NC progenitors underwent apoptosis in both *Foxd3*$^{flox/-}$;*Wnt1-Cre* and *enb5*;*Wnt1-Cre* mutant embryos (Teng et al. 2008; Kam et al. 2014). And this study showed that (1) the expression of *Foxd3* at the dorsal neural tube was reduced in the E9.5 and E10.5 *enb5*;*Wnt1-Cre* mutant mice; and (2) co-electroporation of *enb5* and *Foxd3* drastically reduced the number of *enb5*-induced apoptotic cells in the chick dorsal neural tube. All these suggested that the perturbation of normal *Hoxb5* function in NC would lower the expression of *Foxd3*, which consequently led to apoptosis, and the apoptosis could be prevented upon ectopic expression of *Foxd3*: *Hoxb5* induced *Foxd3* to maintain the survival of NC progenitors. However, in the chick

electroporation experiment, *Hoxb5* could only induce ectopic expression of *Foxd3* at the dorsal neural tube. In addition, section *in situ* hybridization analyses revealed that *Hoxb5* transcripts were detected from the dorsal to ventral neural tube (unpublished data), and *Foxd3* expression was restricted to the dorsal neural tube from where NC was generated (Labosky and Kaestner 1998; Dottori et al. 2001). It was therefore apparent that *Hoxb5* alone was not sufficient to induce *Foxd3*, and only the prospective NC progenitors at the dorsal neural tube were receptive to *Hoxb5* induction. In other words, Hoxb5 must cooperate with other signals and/or transcription factor(s) to induce *Foxd3* expression in the prospective NC progenitors.

Integration of signal gradients of the bone morphogenetic proteins (Bmp), fibroblast growth factors, Wnt and Sonic hedgehog (Shh) along the dorsal-ventral axes of the neural tube are critical in the patterning of the neural tube, and that the NC progenitors are only induced at the dorsal neural tube where the neural tube cells are exposed to the highest concentrations of Bmp and Wnt (Stuhlmiller and Garcia-Castro 2012; Liu et al. 2013; Sasai et al. 2014). Bmp and Notch signalings were required for the NC induction by *Hoxb1* in the chick neural tube, which suggested that *Hoxb1* gene interacted with Bmp signal in the NC induction (Gouti et al. 2011). It is possible that Hoxb5 interacts with Bmp signal in the induction of *Foxd3*, and only those prospective NC progenitors at the dorsal neural tube that are exposed to high Bmp

signal are receptive to Hoxb5.

The lack of defects in the NC-derived tissues in *Hoxb5*$^{-/-}$ mice could be due to functional redundancy among paralogous *Hox* members such as *Hoxa5* and *Hoxc5* (Rancourt et al. 1995). *Hoxa5*, *Hoxb5* and *Hoxc5* paralog genes share some common target genes and common functions for the development with one of the *Hox5* paralog genes playing a predominant role (Boucherat et al. 2013; Xu et al. 2013). *Hoxa5* and *Hoxc5* could induce luciferase activity from the *FOXD3 (wt)-Luc* reporter construct, albeit to a much lesser extent; and their inductions could be blocked by enb5 too (unpublished data). Although *Hoxa5*, *Hoxb5* and *Hoxc5* genes were sharing some functions in the regulation of *Foxd3*, *Hoxb5* was still playing a predominant role. Respective to this observation, it is plausible that enb5 predominantly perturbed the function of *Hoxb5*, but enb5 might also interfere with the functions of other paralogous *Hox* genes such as *Hoxa5* and *Hoxc5* in the NC development. In future, mutant mice carrying a loss-of-function mutation of the transactivation domain of Hoxb5 could be generated to specifically and directly investigate the functions of *Hoxb5* in the embryonic development.

NC migrates from different regions along the A-P axis of the neural tube to form different structures, and the defective NC development affects multiple tissues and causes congenital human diseases. The genetic etiology of many of these diseases is

still poorly understood. Current and previous studies indicated that *Hoxb5* regulated the expression of NC specifiers *Foxd3* and *Sox9* in the early NC, and the perturbation of Hoxb5 function led to the reduction of *Foxd3* and *Sox9* expressions and multiple NC developmental defects (Kam et al. 2014). Therefore, abnormal Hoxb5 function could disturb the molecular cascades between signaling inputs, neural plate border genes and NC specifiers, leading to multiple NC developmental defects.

## 5. Conclusions

Current study shows Hoxb5 binds to the promoter of *Foxd3*, a well-known NC specifier and survival gene, thereby trans-activates *Foxd3* expression and regulates the NC development.

**Figure legends**

**Fig. 1** HOXB5 bound and trans-activated the human *FOXD3* promoter. (A) The human *FOXD3* promoter sequence and nucleotides were numbered with the transcription start site as 1. The putative HOX binding sequence (box) with the core binding sequence in bold was indicated. Dotted line demarcated the promoter fragment for EMSA. Arrows denoted primers for the quantitative PCR. (B) EMSA for HOXB5 binding to *FOXD3* promoter. "+" or "-" indicated the presence or absence of a reagent in EMSA. The amount of the unlabeled fragment (Cold probe) added in the competition assay was 300-folds of the amount of the labeled probe. (C) ChIP and quantitative PCR for HOXB5 binding to *FOXD3* promoter in transfected neuroblastoma cell line (SK-N-SH). y-axis indicated fold of enrichment (mean±SEM) normalized to control IgG. (D) HOXB5 trans-activation from the wild-type *FOXD3* promoter (*FOXD3* (*wt*)-*Luc*) and mutated promoter with the deletion of the HOX binding site (*FOXD3* (*del*)-*Luc*). Fold changes (mean±SD) were determined relative to luciferase unit of *pRC/CMV*. "+" or "-" indicated the presence or absence of a reagent in the reaction mixtures.

**Fig. 2** Hoxb5 bound to the *Foxd3* promoter in mouse. (A) Human (upper) and mouse (lower) *FOXD3* promoter sequences with the putative HOX binding sequences (box) indicated. Arrows denoted primers for the quantitative PCR. (B) ChIP and quantitative PCR for the Hoxb5 binding to *Foxd3* promoter in the central nervous system of E9.5

mouse embryos. y-axis indicated fold of enrichment (mean±SEM) normalized to control IgG.

**Fig. 3** HOXB5 trans-activation from the human *FOXD3* promoter was suppressed by the dominant-negative chimera, enb5. (A) HOXB5 trans-activation from the human *FOXD3* promoter (*FOXD3-Luc*) with or without enb5 inhibition. Fold of increment (mean±SD) was determined relative to the luciferase unit of *pRC/CMV*. (B) Trans-activation of human *FOXD3* promoter (*FOXD3-Luc*) by HOXB5 with or without Flag-enb5. The relative luciferase activity in cells transfected with *HOXB5* alone was arbitrarily regarded as 100%. (C) ChIP and quantitative PCR for Flag-enb5 binding to the human *FOXD3* promoter. y-axis indicated fold of enrichment (mean±SEM) normalized to control IgG.

**Fig. 4** Reduction of *Foxd3* expression in *enb5*;*Wnt1-Cre* mice. Transcripts of *Foxd3* (purple) in (A) E9.5 and (C) E10.5 *enb5* (wt control) and *enb5*;*Wnt1-Cre* embryos were localized by whole mount *in situ* hybridization. (B) The relative expressions of *Foxd3* in the neural tubes of the E9.5 *enb5* (filled bar) and *enb5*;*Wnt1-Cre* embryos (unfilled bar) were calculated and shown as mean±SEM, with the expression of *Foxd3* in the *enb5* neural tubes taken arbitrarily as one. Number of neural tubes analyzed was indicated by “n”. (D) Foxd3-expressing cells (green) were localized in the E9.5 *enb5* (wt control) and *enb5*;*Wnt1-Cre* embryos by immuno-fluorescence

using anti-Foxd3 serum. Regions highlighted were magnified and shown as insets. The number of migratory Foxd3+ve cells on the sections of the *enb5* (filled bar) and *enb5;Wnt1-Cre* (unfilled bar) mice were counted and shown as mean±SD. Number of embryos analyzed was indicated by "n". Abbreviations: mb, midbrain; hb, hindbrain; h, heart; flb, forelimb bud; nt, neural tube; cv, cardinal vein; da, dorsal aorta; se, surface ectoderm; fgt, foregut.

**Fig. 5** Foxd3 alleviated enb5-induced cell death and *Hoxb5* induced *Foxd3* expression in chick neural tube. (A) *In ovo* electroporation with *enb5* and chick *Foxd3*, either alone or in combination. Chick neural tubes were assayed for TUNEL (red) and immuno-fluorescence for GFP (green) 24 hours post-transfection. Number of embryos analyzed was indicated by "n". (B) The percentage of the transfected cells (GFP+ve; green) that underwent apoptosis (TUNEL+ve; red) in the neural tubes electroporated with *enb5* and chick *Foxd3*, either alone or together were determined and shown as mean±SEM. Number of embryos analyzed was indicated by "n". (C) Chick neural tubes electroporated with chick *Hoxb5* were assayed for GFP (green) and *Foxd3* expression by *in situ* hybridization (*ISH*; purple) 12 hours post-transfection. GFP immuno-reactivity (green) indicated that the region of the neural tube transfected with *Hoxb5*. Dotted line demarcated the ectopic expression of *Foxd3* in the *Hoxb5* transfected neural tube. (n/n) indicated number of embryos showing positive detection

(GFP or *Foxd3*) versus number of transfected embryos.

**Acknowledgements**

Anti-Foxd3 serum was provided as a gift by Prof. Patricia A Labosky (Vanderbilt University Medical Center, USA); the human *FOXD3*-lucifrease reporting vector [*FOXD3* (*wt*)-*Luc*] was kindly provided by Prof. Richard A. Spritz (University of Colorado Denver, Aurora, USA); the mouse *Foxd3* plasmid for synthesizing riboprobe was provided by Dr. Ruth Arkell (Laboratory of Early Development, Mammalian Genetics Unit, MRC, Harwell, UK). The *Wnt1-Cre* mice were provided by Prof. Andrew P. McMahon (Harvard University, USA). This work was partly supported by the Hong Kong RGC GRF (HKU 7245/02M) and HKU Seed Funding for Basic Research (200811159088) to VCH Lui.

**References:**


Alkhateeb A, Fain PR, Spritz RA. 2005. Candidate functional promoter variant in the FOXD3 melanoblast developmental regulator gene in autosomal dominant vitiligo. *The Journal of investigative dermatology* **125**: 388-391.

Boucherat O, Montaron S, Berube-Simard FA, Aubin J, Philippidou P, Wellik DM, Dasen JS, Jeannotte L. 2013. Partial functional redundancy between Hoxa5 and Hoxb5 paralog genes during lung morphogenesis. *Am J Physiol Lung Cell Mol Physiol* **304**: L817-830.

Cheung M, Chaboissier MC, Mynett A, Hirst E, Schedl A, Briscoe J. 2005. The transcriptional control of trunk neural crest induction, survival, and delamination. *Dev Cell* **8**: 179-192.

del Barrio MG, Nieto MA. 2002. Overexpression of Snail family members highlights their ability to promote chick neural crest formation. *Development* **129**: 1583-1593.

Dottori M, Gross MK, Labosky P, Goulding M. 2001. The winged-helix transcription factor Foxd3 suppresses interneuron differentiation and promotes neural crest cell fate. *Development* **128**: 4127-4138.

Fu M, Lui VC, Sham MH, Cheung AN, Tam PK. 2003. HOXB5 expression is spatially and temporarily regulated in human embryonic gut during neural crest cell colonization and differentiation of enteric neuroblasts. *Dev Dyn* **228**: 1-10.

Gavalas A, Studer M, Lumsden A, Rijli FM, Krumlauf R, Chambon P. 1998. Hoxa1 and Hoxb1 synergize in patterning the hindbrain, cranial nerves and second pharyngeal arch. *Development* **125**: 1123-1136.

Gendron-Maguire M, Mallo M, Zhang M, Gridley T. 1993. Hoxa-2 mutant mice exhibit homeotic transformation of skeletal elements derived from cranial neural crest. *Cell* **75**: 1317-1331.

Gouti M, Briscoe J, Gavalas A. 2011. Anterior Hox genes interact with components of the neural crest specification network to induce neural crest fates. *Stem Cells* **29**: 858-870.

Hogan BL, Holland PW, Lumsden A. 1988. Expression of the homeobox gene, Hox 2.1, during mouse embryogenesis. *Cell Differ Dev* **25 Suppl**: 39-44.

Holland PW, Hogan BL. 1988. Spatially restricted patterns of expression of the homeobox-containing gene Hox 2.1. during mouse embryogenesis. *Development* **102**: 159-174.

Kam MK, Cheung MC, Zhu JJ, Cheng WW, Sat EW, Tam PK, Lui VC. 2014. Perturbation of Hoxb5 signaling in vagal and trunk neural crest cells causes

apoptosis and neurocristopathies in mice. *Cell death and differentiation* **21**: 278-289.

Kessel M. 1993. Reversal of axonal pathways from rhombomere 3 correlates with extra Hox expression domains. *Neuron* **10**: 379-393.

Knecht AK, Bronner-Fraser M. 2002. Induction of the neural crest: a multigene process. *Nat Rev Genet* **3**: 453-461.

Krumlauf R, Holland PW, McVey JH, Hogan BL. 1987. Developmental and spatial patterns of expression of the mouse homeobox gene, Hox 2.1. *Development* **99**: 603-617.

Kuratani SC, Wall NA. 1992. Expression of Hox 2.1 protein in restricted populations of neural crest cells and pharyngeal ectoderm. *Dev Dyn* **195**: 15-28.

Labosky PA, Kaestner KH. 1998. The winged helix transcription factor Hfh2 is expressed in neural crest and spinal cord during mouse development. *Mech Dev* **76**: 185-190.

Liu JA, Wu MH, Yan CH, Chau BK, So H, Ng A, Chan A, Cheah KS, Briscoe J, Cheung M. 2013. Phosphorylation of Sox9 is required for neural crest delamination and is regulated downstream of BMP and canonical Wnt signaling. *Proc Natl Acad Sci U S A* **110**: 2882-2887.

Lui VC, Cheng WW, Leon TY, Lau DK, Garcia-Barcelo MM, Miao XP, Kam MK, So MT, Chen Y, Wall NA et al. 2008. Perturbation of hoxb5 signaling in vagal neural crests down-regulates ret leading to intestinal hypoganglionosis in mice. *Gastroenterology* **134**: 1104-1115.

Makki N, Capecchi MR. 2011. Identification of novel Hoxa1 downstream targets regulating hindbrain, neural crest and inner ear development. *Dev Biol* **357**: 295-304.

Mallo M, Wellik DM, Deschamps J. 2010. Hox genes and regional patterning of the vertebrate body plan. *Dev Biol* **344**: 7-15.

Meulemans D, Bronner-Fraser M. 2004. Gene-regulatory interactions in neural crest evolution and development. *Dev Cell* **7**: 291-299.

Mundell NA, Labosky PA. 2011. Neural crest stem cell multipotency requires Foxd3 to maintain neural potential and repress mesenchymal fates. *Development* **138**: 641-652.

Nieto MA. 2002. The snail superfamily of zinc-finger transcription factors. *Nat Rev Mol Cell Biol* **3**: 155-166.

Niwa H, Yamamura K, Miyazaki J. 1991. Efficient selection for high-expression transfectants with a novel eukaryotic vector. *Gene* **108**: 193-199.

Rancourt DE, Tsuzuki T, Capecchi MR. 1995. Genetic interaction between hoxb-5 and hoxb-6 is revealed by nonallelic noncomplementation. *Genes Dev* **9**:

108-122.

Rijli FM, Mark M, Lakkaraju S, Dierich A, Dolle P, Chambon P. 1993. A homeotic transformation is generated in the rostral branchial region of the head by disruption of Hoxa-2, which acts as a selector gene. *Cell* **75**: 1333-1349.

Sasai N, Kutejova E, Briscoe J. 2014. Integration of Signals along Orthogonal Axes of the Vertebrate Neural Tube Controls Progenitor Competence and Increases Cell Diversity. *PLoS Biol* **12**: e1001907.

Studer M, Gavalas A, Marshall H, Ariza-McNaughton L, Rijli FM, Chambon P, Krumlauf R. 1998. Genetic interactions between Hoxa1 and Hoxb1 reveal new roles in regulation of early hindbrain patterning. *Development* **125**: 1025-1036.

Stuhlmiller TJ, Garcia-Castro MI. 2012. Current perspectives of the signaling pathways directing neural crest induction. *Cell Mol Life Sci* **69**: 3715-3737.

Sutton J, Costa R, Klug M, Field L, Xu D, Largaespada DA, Fletcher CF, Jenkins NA, Copeland NG, Klemsz M et al. 1996. Genesis, a winged helix transcriptional repressor with expression restricted to embryonic stem cells. *J Biol Chem* **271**: 23126-23133.

Teng L, Mundell NA, Frist AY, Wang Q, Labosky PA. 2008. Requirement for Foxd3 in the maintenance of neural crest progenitors. *Development* **135**: 1615-1624.

Wall NA, Jones CM, Hogan BL, Wright CV. 1992. Expression and modification of Hox 2.1 protein in mouse embryos. *Mech Dev* **37**: 111-120.

Xu B, Hrycaj SM, McIntyre DC, Baker NC, Takeuchi JK, Jeannotte L, Gaber ZB, Novitch BG, Wellik DM. 2013. Hox5 interacts with Plzf to restrict Shh expression in the developing forelimb. *Proc Natl Acad Sci U S A* **110**: 19438-19443.

Zhu J, Garcia-Barcelo MM, Tam PK, Lui VC. 2011. HOXB5 cooperates with NKX2-1 in the transcription of human RET. *PLoS One* **6**: e20815.

**Figure 1**

Click here to download high resolution image

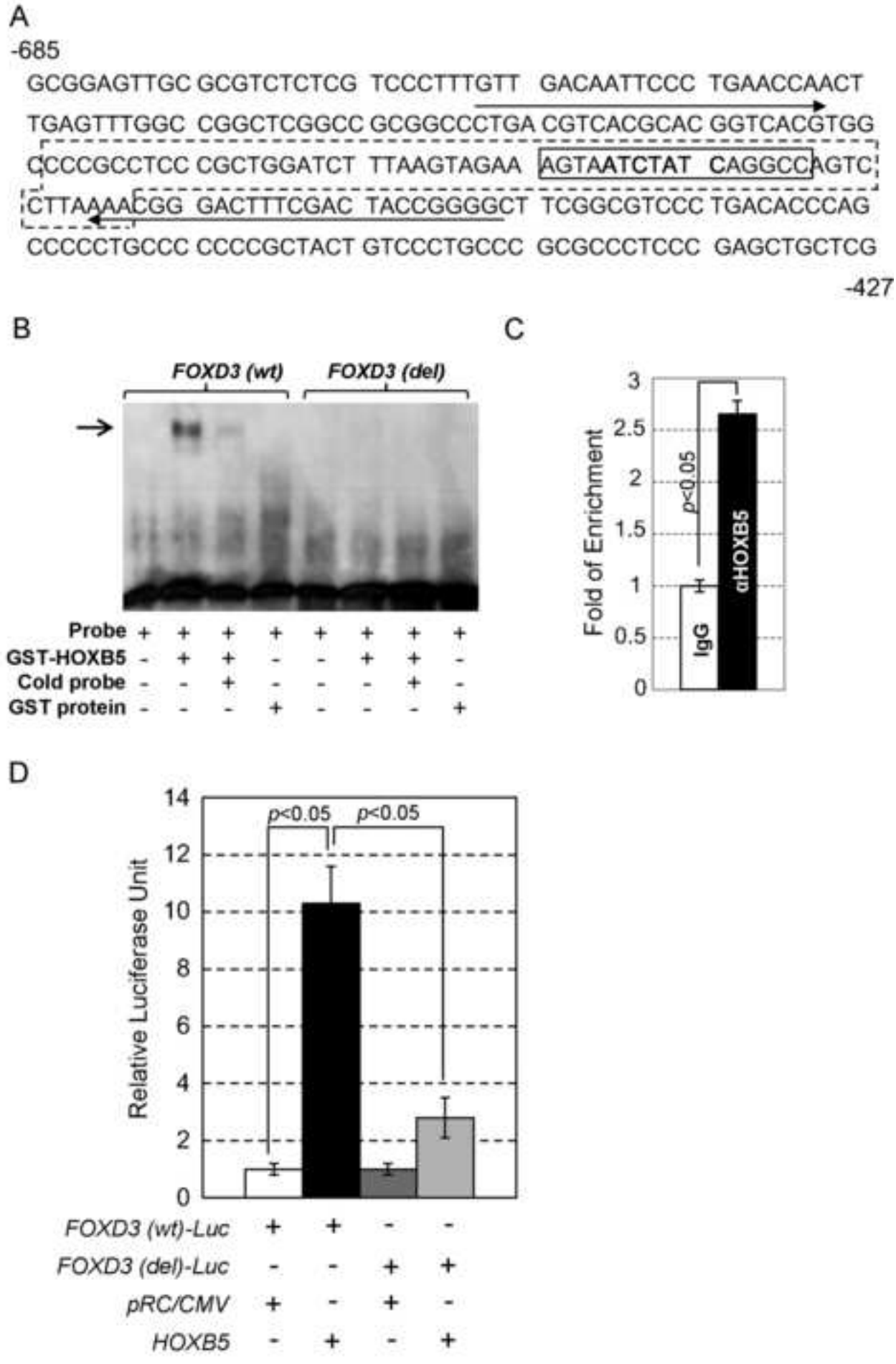

Figure 2

Click here to download high resolution image

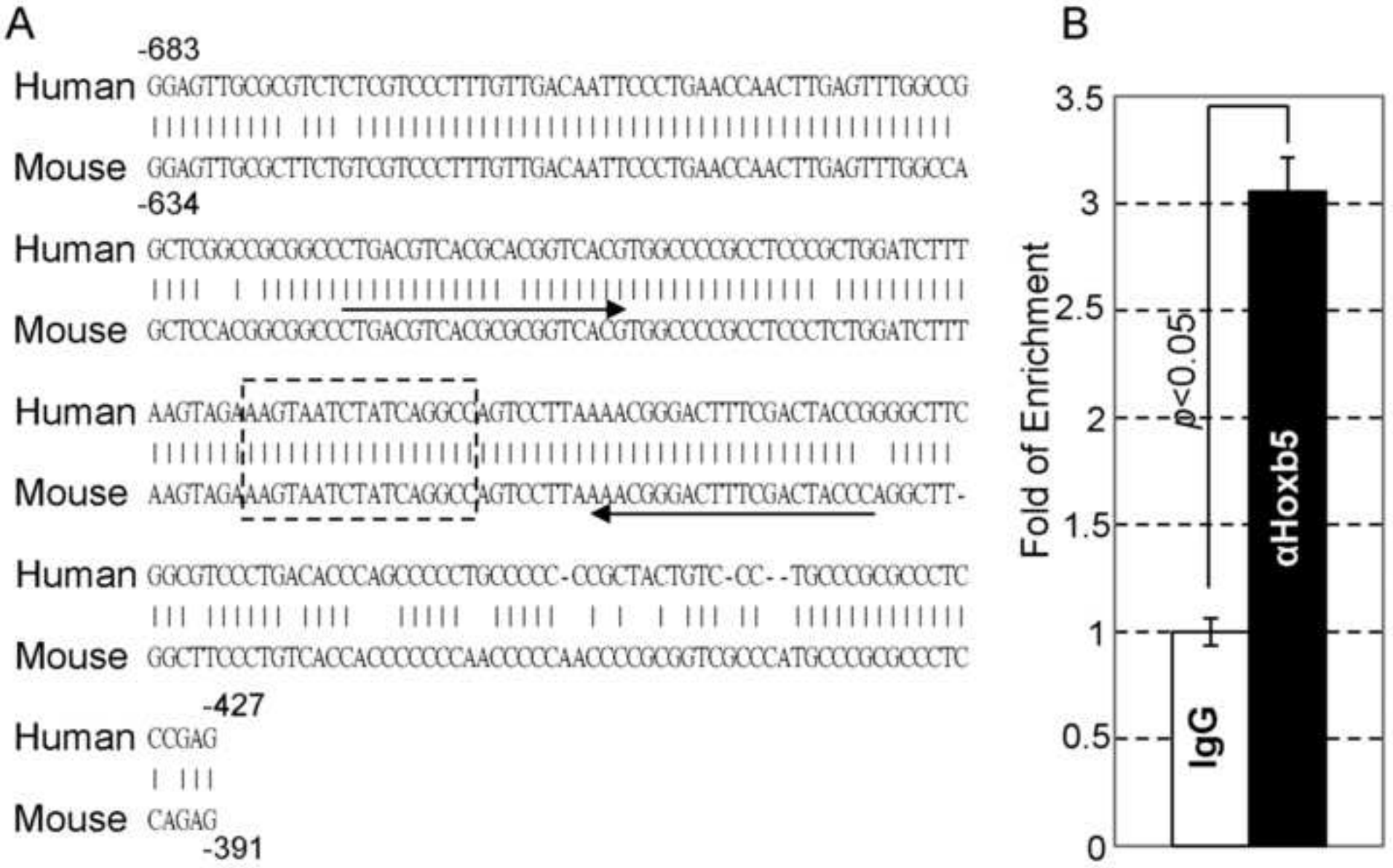

Figure 3

Click here to download high resolution image

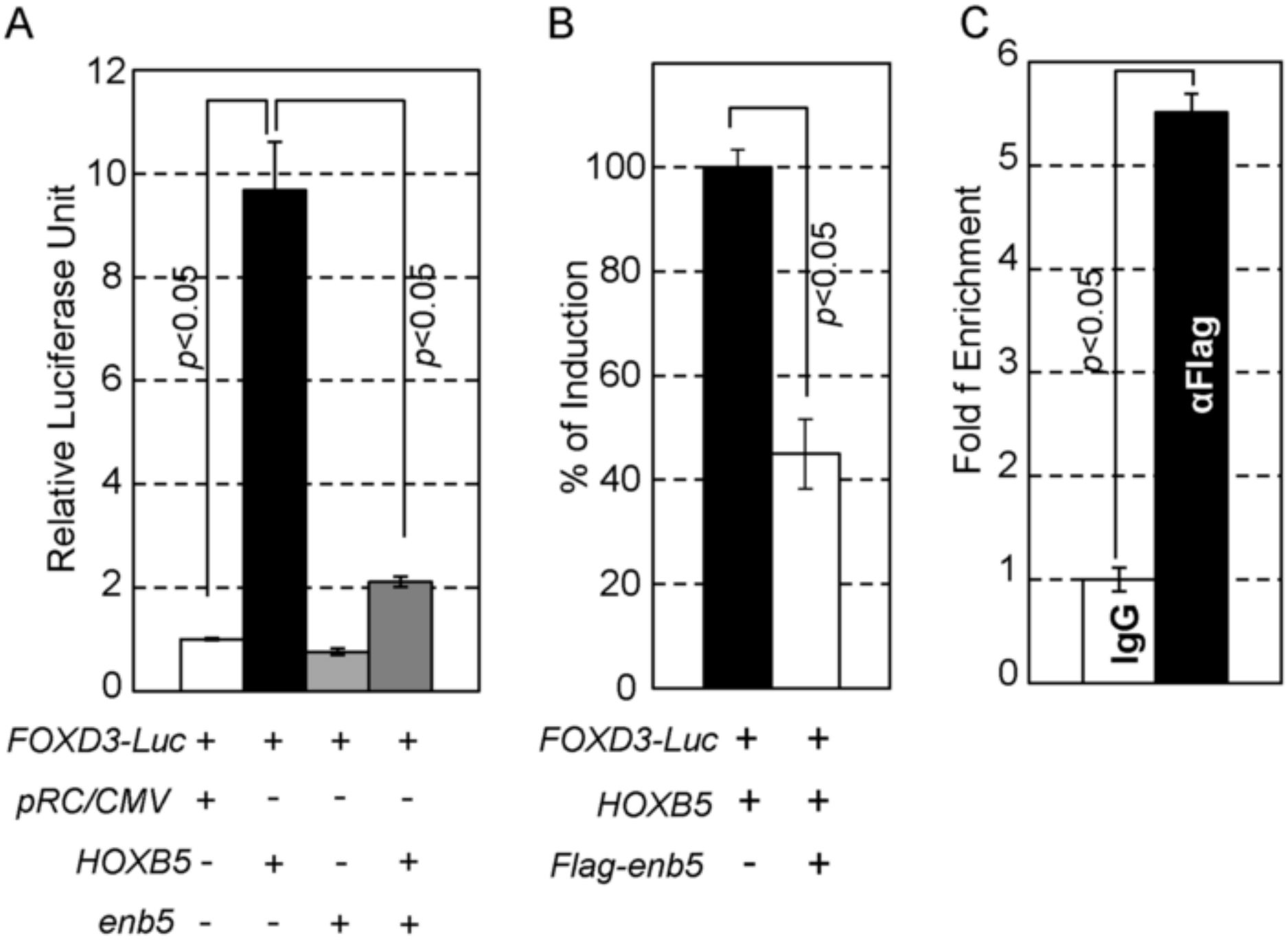

**Figure 4**

Click here to download high resolution image

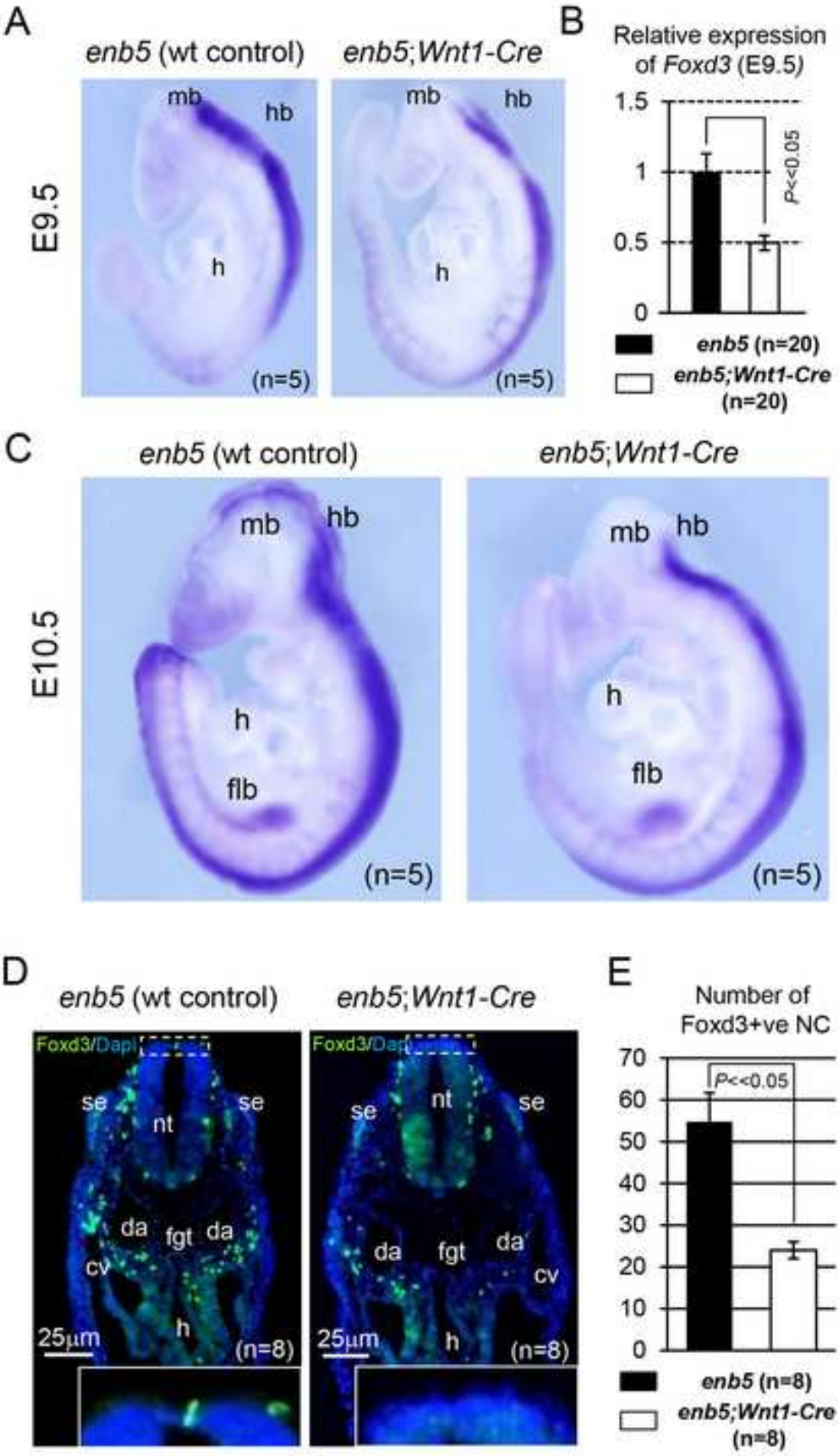

**Figure 5**

Click here to download high resolution image